

## SURFACE ANALYSIS OF ELECTROCHROMIC $\text{Cu}_x\text{O}$ FILMS IN THEIR COLORED AND BLEACHED STATES

### POVRŠINSKA ANALIZA ELEKTROKROMIZNIH PLASTI $\text{Cu}_x\text{O}$ V NJIHOVIH OBARVANIH IN OBELJENIH STANJIH

Mimoza M. Ristova<sup>1,2</sup>, Milorad Milun<sup>3</sup>, Biljana Pejova<sup>4</sup>

<sup>1</sup>Faculty of Natural Sciences and Mathematics, Institute of Physics, P.O. Box 162, Skopje, R. Macedonia

<sup>2</sup>Materials Science Division, Lawrence Berkeley National Laboratory, Berkeley, CA, USA

<sup>3</sup>Institute of Physics, Bijenicka Cesta 46, Zagreb, Croatia

<sup>4</sup>Faculty of Natural Sciences and Mathematics, Institute of Chemistry, P.O. Box 162, Skopje, R. Macedonia  
mima.ristova@gmail.com

*Prejem rokopisa – received: 2014-06-25; sprejem za objavo – accepted for publication: 2014-07-04*

doi:10.17222/mit.2014.092

$\text{Cu}_x\text{O}$  is known as an electrochromic material with a possible applicability for solar-light modulation. The reversible transition between the two different oxidation states,  $\text{CuO}$  and  $\text{Cu}_2\text{O}$ , is responsible for the visible-light switching ability.  $\text{Cu}_x\text{O}$  films in their as-prepared, colored and bleached states were subjected to a surface analysis in order to relate the bleaching/coloring effects to the quantified Cu-oxide transition. An XPS analysis on the  $\text{Cu}2p$  electrons of the as-prepared, bleached and colored films showed that the Cu-ion quantity reversibly turning from  $\text{CuO}$  to  $\text{Cu}_2\text{O}$  during the electrochromic cycling was about 3.4 %. An analysis of the XRD patterns of the film's three states confirmed that a small portion of the surface Cu-atoms probably participate in the coloration/bleaching process. Scanning electron microscopy (SEM) images revealed obvious changes in the surface morphology due to bleaching and coloration transitions, particularly in the grain size and porosity of the  $\text{Cu}_x\text{O}$  films. The surface morphology of the films was also studied with the atomic force microscopy (AFM). This technique allowed significant conclusions to be derived relating to the surface roughness as well as the compositional homogeneity of the films before and after electrochemical treatments. These results appeared to be complementary to those derived from the X-ray diffraction patterns. One may assume that the coloration centers are located at very few film's monolayers of the interface with the electrolyte.

Keywords: electrochromism,  $\text{Cu}_x\text{O}$ ,  $\text{CuO}$ , XPS, XRD, SEM, AFM

$\text{Cu}_x\text{O}$  je poznan kot elektrokromizni material z možnostjo uporabe za modulacijo sončne svetlobe. Reverzibilni prehod med dvema oksidacijskima stanjema,  $\text{CuO}$  in  $\text{Cu}_2\text{O}$ , vpliva na možnost preklapljanja vidne svetlobe. Tanke plasti  $\text{Cu}_x\text{O}$  v izhodnem, obarvanem ali obeljenem stanju so bile analizirane na površini, da bi ugotovili učinke barvanja/beljenja pri kvantificiranem prehodu Cu-oksidov. XPS-analiza z elektroni  $\text{Cu}2p$  pripravljene, obeljene in obarvane plasti je pokazala, da se okrog 3,4 % količine Cu-ionov med elektrokromizno obdelavo reverzibilno odmika od  $\text{CuO}$  proti  $\text{Cu}_2\text{O}$ . Analiza XRD-sledov treh stanj traku je potrdila, da verjetno majhen delež Cu-atomov sodeluje v postopku obarvanje/beljenje. Vrstična elektronska mikroskopija (SEM) je potrdila občutne spremembe v morfologiji površine zaradi prehodov obarvanja in obeljenja, posebno velikost zrn in poroznost plasti  $\text{Cu}_x\text{O}$ . Morfologija površine plasti je bila pregledana z mikroskopijo na atomsko silo (AFM). Ta tehnika omogoča pomembne sklepe glede površinske hrapavosti, kot tudi homogenosti sestave plasti pred elektrokemijsko obdelavo in po njej. Ti rezultati se ujemajo s tistimi, dobljenimi z XRD-posnetkov. Lahko sklepamo, da so centri obarvanja locirani v nekaj monoplasteh na stiku z elektrolitom.

Ključne besede: elektrokromizem,  $\text{Cu}_x\text{O}$ ,  $\text{CuO}$ , XPS, XRD, SEM, AFM

## 1 INTRODUCTION

Electrochromic materials are known as modulators of the reflection/transmission of the incident illumination<sup>1</sup>. There are many applications of electrochromic films, one of the most important being the production of large-area electrochromic displays<sup>2</sup>. Rear-view mirrors with a variable reflectance, based on electrochromic oxide films, are commercially available for many kinds of vehicles<sup>2</sup>. The most attractive, very useful and environmental friendly applications of electrochromic materials are the so-called "smart windows"<sup>3</sup> that are able to automatically modulate the incoming solar illumination in the interior. Smart windows may also be alternatively powered by photovoltaic cells, thus, operating as energetically independent devices.

A copper (I) oxide ( $\text{Cu}_2\text{O}$ ) thin film has been a subject of research in numerous studies, as a candidate for a

solar cell application<sup>4</sup>. It is known that copper oxide thin films exhibit cathode electrochromism<sup>5-8</sup>, i.e., they are transparent for visible light in their oxidized state and almost black in their reduced state.

Thin  $\text{Cu}_x\text{O}$  films can be deposited with different techniques: sputtering<sup>8</sup>, electrochemical deposition<sup>9,10</sup>, sol-gel-like dip technique<sup>5,11</sup>, thermal oxidation<sup>12</sup>, anode oxidation<sup>13</sup> or chemical-deposition method<sup>14-17</sup>. Chemically deposited  $\text{Cu}_x\text{O}$  films were the subject of our previous research<sup>17</sup> and are the topic of our present interest. Our former publication<sup>18</sup> showed some of the advantages and disadvantages of this electrochromic material for solar-light-modulation applications, implying the necessity for a more profound surface examination of their light-switching mechanism.

## 2 EXPERIMENTAL WORK

### 2.1 Electrochromic $\text{Cu}_x\text{O}$ film preparation

Fluorine-doped tin oxide films on glass (FTO) with a sheet resistance of 10–20  $\Omega$  and transmittance for the visible light of about 80–85 %, products of Solar-Split, Croatia, were used as the substrates. Electrochromic  $\text{Cu}_x\text{O}$  films were deposited with the electroless-chemical-bath deposition method, described elsewhere<sup>15–17</sup>. The thickness of  $\text{Cu}_x\text{O}$  was estimated from the SEM image of the cross-section of the glass/film interface.

### 2.2 Surface analysis of the $\text{Cu}_2\text{O}$ electrochromic films

The X-ray diffraction patterns of the  $\text{Cu}_x\text{O}$  films on the  $\text{SnO}_2$  (FTO) substrates in their as-prepared, bleached and colored states were recorded with a Rigaku Ultima IV X-ray diffractometer, using  $\text{Cu-K}\alpha$  radiation of 0.15418 nm. XRD scans were taken within an angular interval  $2\theta$  from 20 ° to 70 ° via a step method applying 0.02 ° steps ( $2\theta$ ) and a counting time of 0.6 s per scan. Scattered X-ray radiation was detected using a DteX detector. The XRD pattern of the FTO ( $\text{SnO}_2$ ) substrate was recorded as well. In addition to the identification, the XRD patterns were also used for estimating the average crystal size with the Scherrer method.

The X-ray photoelectron spectroscopy (XPS) instrument consisted of a non-chromatized X-ray source with an Mg-Al dual anode. A hemispherical electrostatic electron analyzer VSW HA100 was employed under the following operating conditions: a fixed-analyzer-transition (FAT) mode of 50 eV and a resolution of 1.1 eV. The XPS spectra were taken from the  $\text{Cu}_x\text{O}$  electrochromic films deposited onto the conductive FTO surface, in their as-prepared, bleached and colored states. The Mg- $\text{K}\alpha$  XPS spectra were taken from the film surfaces with no previous  $\text{Ar}^+$  ion-beam cleaning, taking into account that the electrochromic modifications possibly take place on the immediate surface of the interface with the electrolytes. The binding energy of the Cu2p electrons was subjected to an analysis. Taking into account that the Cu2p electron binding energy shifts due to the presence of various copper-oxygen compounds each of the compounds was quantified.

Scanning electron microscopy (SEM) was used for an estimation of the  $\text{Cu}_x\text{O}$  film thickness by taking the scans from the film/glass substrate cross-section profile. Surface SEM scans were taken from the surface of the  $\text{Cu}_x\text{O}$ /substrate as well as from the sole substrate. The SEM analyses of the scans taken from the  $\text{Cu}_x\text{O}$ /FTO samples in their as-prepared, bleached and colored states were used for depicting the variation in the crystal grain size and the porosity. A digitalized system of JEOL JSM-T220A SEM was used.

The surface morphology and phase composition of the investigated  $\text{Cu}_x\text{O}$  films, in their as-prepared, colored and bleached state, were studied with atomic force microscopy (AFM). The height, amplitude error and

phase images were measured using a scanning probe Shimadzu microscope SPM 9600 operating in a dynamic and phase mode. The measurements were performed using silicon SPM probes with a resonance frequency of 320 kHz and a force constant of 42 N/m. Several different regions on the investigated sample surface were explored. The scan rate was 1 Hz or 2 Hz depending on the size of the scanned area (1  $\mu\text{m}$  or 5  $\mu\text{m}$ ). The image resolution was 512 lines per each scan direction. The measured images were only flattened, without any further processing. The surface roughness was calculated using the SMP Manager data processing software.

## 3 RESULTS AND DISCUSSION

### 3.1 Film bleaching and coloration

Three  $\text{Cu}_x\text{O}$  films were deposited under equal conditions onto the FTO substrate. One of the films was kept in the as-prepared condition for further examination. The second film was brought into the bleached state as it was biased with +1 V against the FTO adjacent electrode in a 0.2 M  $\text{KNO}_3$  solution for 10 seconds. The third film was fully colored upon biasing with –1 V against the FTO adjacent electrode in the 0.2 M  $\text{KNO}_3$  solution for 10 s. The three films were subjected to a surface analysis, described in section 3.2. It is worth mentioning that the films retained their electrochromic colors for a long time (over one year) upon the completion of the surface analysis.

### 3.2 Surface analyses of the $\text{Cu}_x\text{O}$ films (XRD, XPS, SEM and AFM)

The XRD patterns of the  $\text{Cu}_x\text{O}$  electrochromic films, deposited onto the FTO substrate in their as-prepared, bleached and colored state, are presented in **Figure 1**. The  $\text{SnO}_2$  (FTO) substrate alone was also analyzed. The corresponding CPDS files for CuO,  $\text{Cu}_2\text{O}$  and  $\text{SnO}_2$  are given in<sup>19–21</sup>.

As can be seen from **Figure 1**, only three peaks were identified in addition to the one of the  $\text{SnO}_2$  substrate. The analysis showed that all three detectable peaks, low in intensity, pertained to the  $\text{Cu}_2\text{O}$  cuprite phase. The small  $\text{Cu}_2\text{O}$  peak intensity and the absence of the identifiable peaks typical for the tenorite crystalline oxide state of copper (CuO) did not allow us to draw any conclusions about the electrochromic reversible switching between the two Cu-oxide states. Thus, one may speculate that the transition from the bleached to the colored state and its reverse process occur through the known transition of only a minor (sub-detectable) portion of the dominant oxide of  $\text{Cu}_2\text{O}$  into CuO.

The diffraction pattern of the as-prepared  $\text{Cu}_x\text{O}$  sample shows two diffraction peaks between the  $2\theta$  angles of 42 ° and 36 °, which are characteristic for copper (I) oxide. Following the fitting procedure, the angular position and the full width at half maximum (FWHM) of

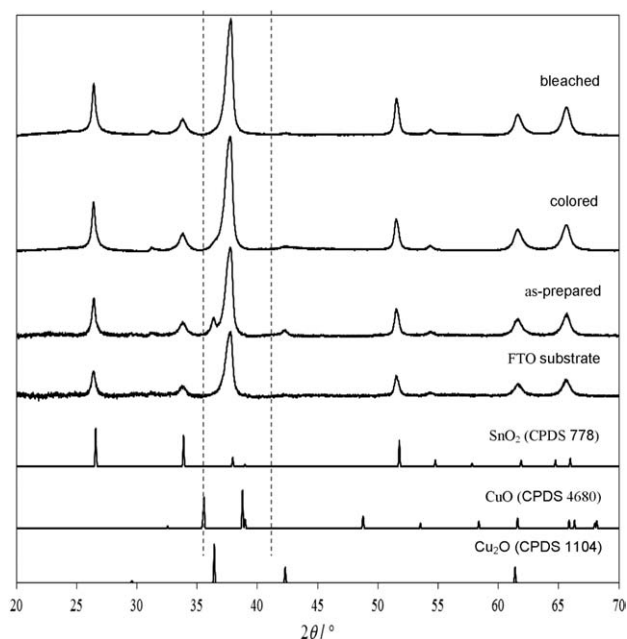
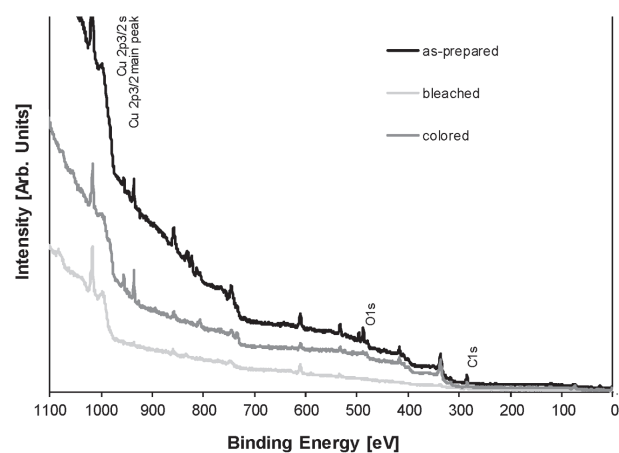


**Figure 1:** XRD patterns of the  $\text{Cu}_x\text{O}$  electrochromic films deposited onto the FTO substrate in their as-prepared, bleached and colored state. The pattern of the substrate and the corresponding CPDS files are given on the graph.

**Slika 1:** XRD-posnetki elektrokromiznih plasti, nanesenih na FTO-podlago v njihovem pripravljenem, obeljenem in obarvanem stanju. Na sliki so prikazani vzorec podlage in ustrezne CPDS-datoteke.

detectable diffraction peaks were found. The average crystal diameter was estimated to be about 24 nm using the Scherrer equation.

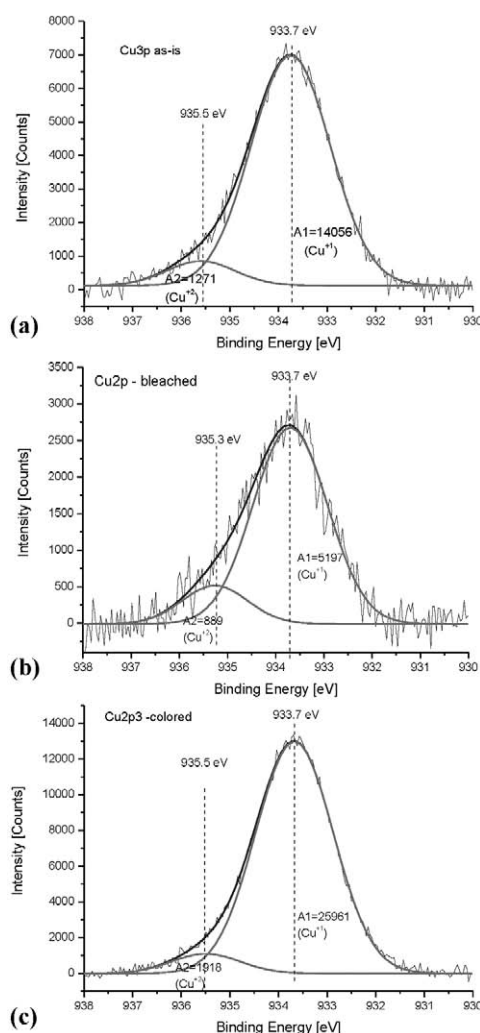
**Figure 2** presents broad XPS spectra of the  $\text{Cu}_x\text{O}$  film in its as-prepared, bleached and colored states. The distinct peaks of the binding energy were found to originate from all the elements of the film compound, such as Cu (the 2p<sub>3/2</sub> main peak centered at around 932 eV and a strong satellite centered at 943 eV), O (O1s) and C (C1s). The expected Auger peak of Cu L<sub>3</sub>M<sub>4,5</sub>M<sub>4,5</sub>



**Figure 2:** Broad XPS spectra of the  $\text{Cu}_x\text{O}$  film in its as-prepared, bleached and colored states

**Slika 2:** Širokopasovni XPS-spekter plasti  $\text{Cu}_x\text{O}$  v pripravljenem, obeljenem in obarvanem stanju

is not sufficiently distinct on either of the three sample broad spectra). The three Cu2p<sub>3/2</sub> spectra were corrected by fixing the C1s peak to 285 eV. Each of the corrected XPS Cu2p<sub>3/2</sub> spectra was then deconvoluted into two Gaussian peaks corresponding to CuO, known to appear between 934.2 eV<sup>22–24</sup> and 935.2 eV<sup>21</sup>, and to Cu<sub>2</sub>O, known to appear between 932.3 eV and 933.8 eV<sup>22–25</sup>. Since the Cu<sup>0</sup> and Cu<sub>2</sub>O Cu2p<sub>3/2</sub> peaks can not be resolved with deconvolution (the binding energy shift between the two is only about 0.1 eV)<sup>24</sup>, Cu(OH)<sub>2</sub> can not be clearly distinguished from CuO at 935.3 eV<sup>22</sup> due to their overlap. Disregarding the presence of the copper metal and hydroxide, we can assume that the entire Cu2p signal originates from the CuO and Cu<sub>2</sub>O compounds. Each of the two Gaussian-peak areas (A1 and A2) of the Cu2p<sub>3/2</sub> zero-leveled XPS spectra on **Figure 3** is proportional to

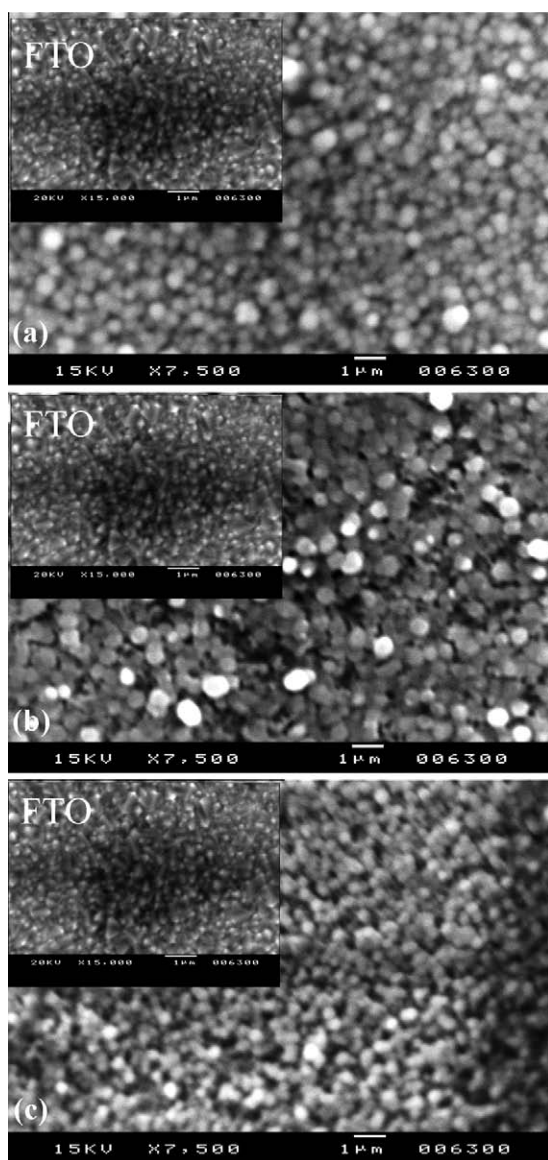


**Figure 3:** Deconvolution of the XPS spectra of Cu2p<sub>3</sub> electrons on two Gaussian peaks: a) as-prepared, b) bleached and c) colored electrochromic  $\text{Cu}_x\text{O}$  film on FTO substrates. A1 and A2 are the corresponding peak areas.

**Slika 3:** Upadanje XPS-spektra elektronov Cu2p<sub>3</sub> na dveh Gaussovih vrhovih: a) pripravljene, b) obeljene in c) obarvane elektrokromizne plasti  $\text{Cu}_x\text{O}$  na FTO-podlagi. A1 in A2 sta odgovarjajoči področji vrhov.

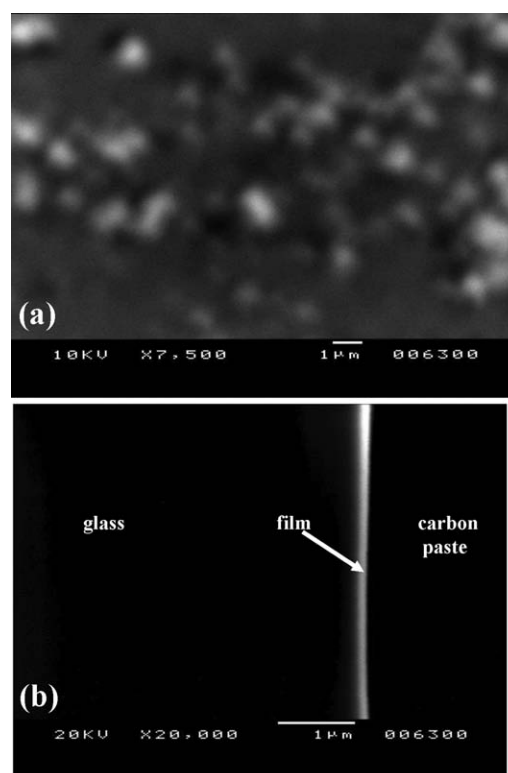
**Table 1:** Binding energies of Cu2p<sub>3/2</sub> electrons, obtained from XPS spectra with deconvolution on two Gaussian peaks with areas A1 and A2. Reference values are given for comparison.**Tabela 1:** Energije vezav elektronov Cu2p<sub>3/2</sub>, dobljenih iz XPS-spektra z dekonvolucijo v dva Gaussova vrhova A1 in A2. Za primerjavo so prikazane referenčne vrednosti.

	B. E. Cu2p in Cu <sup>+2</sup> bonding (as in CuO) (eV)	B. E. Cu2p in Cu <sup>+1</sup> bonding (as in Cu <sub>2</sub> O) (eV)	ΔB. E. (eV)	Fraction of Cu <sup>+2</sup> (as in CuO) of the total Cu atoms A2/(A1+A2) (%)	Fraction of Cu <sup>+1</sup> (as in Cu <sub>2</sub> O) of the total Cu atoms =A1/(A1+A2) (%)
XPS handbook <sup>22</sup>	933.6				
Literature –XPS native oxides <sup>23</sup>	934.2	932.5	1.7	22.1	77.9
T. Ghodselahe et al. <sup>24</sup>	934.5–935.2	932.3–933.8	1.4–2.2		
I. G. Casella et al. <sup>25</sup>		932.2–932.8			
As-prepared	935.5	933.7	1.8	9.8	90.2
Colored	935.5	933.7	1.8	6.8	93.2
Bleached	935.3	933.7	1.6	10.2	89.8

**Figure 4:** SEM micrographs taken of the surfaces of the: a) as-prepared, b) bleached and c) colored films on FTO substrates**Slika 4:** SEM-posnetki površine plasti na FTO-podlagi: a) pripravljeno, b) obeljeno in c) obarvano

the signal yield from the Cu atoms bonded in either CuO or Cu<sub>2</sub>O. Hence, the relative peak area of either A1 or A2 versus the total peak area (A1+A2) in percent can be considered a measure for the Cu<sup>+1</sup> (as in CuO) and Cu<sup>+2</sup> (as in Cu<sub>2</sub>O) quantities in the film. A possible presence of the elemental copper and hydroxide was neglected because these are not active participants in the reversible electrochromic redox reactions.

The results for the Cu2p binding energies of the three states of the electrochromic Cu<sub>x</sub>O film from **Figure 3** are

**Figure 5:** a) SEM of the Cu<sub>x</sub>O film grown on an amorphous substrate (glass), b) SEM of the cross-section of the Cu<sub>x</sub>O film on a glass interface. The estimated film thickness is about 250 nm.**Slika 5:** a) SEM-posnetek Cu<sub>x</sub>O filma, nastalega na amorfni podlagi (steklo), b) SEM-posnetek prereza plasti Cu<sub>x</sub>O na steklu. Debelina plasti je okrog 250 nm.

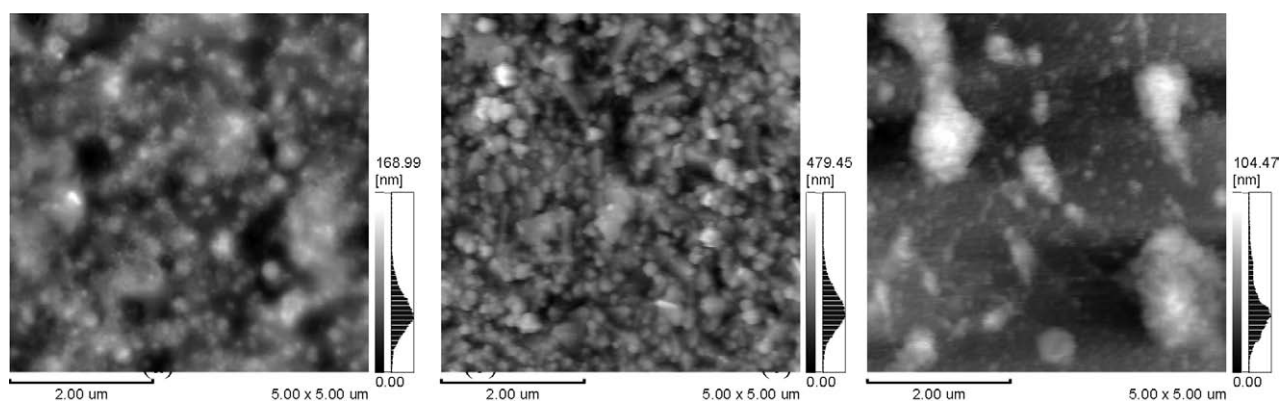


**Figure 6:** Two-dimensional surface images of: a) as-prepared, b) colored and c) bleached  $\text{Cu}_x\text{O}$  thin films

**Slika 6:** Dvodimenzionalni posnetek površine tanke plasti  $\text{Cu}_x\text{O}$ : a) pripravljeno, b) obarvano in c) obeljeno

summarized in **Table 1**. It is evident that the experimental values revealed somewhat greater binding energies (about 1.2 eV) than those reported for the bulk samples<sup>23</sup>, but they are in good agreement with those reported for the films<sup>24,25</sup>. The results showed that the binding energies pertaining to the two  $\text{Cu}2p_{3/2}$  peaks retained the known difference of about 1.7 eV<sup>23,24</sup>.

From **Table 1** it is clear that the as-prepared sample contained 90.2 %  $\text{Cu}^{+1}$  (bonded as in  $\text{Cu}_2\text{O}$ , the yellowish transparent oxide). From this point, it is evident that the amount of  $\text{Cu}^{+1}$  slightly increased in the bleached sample, up to 93.2 %, but decreased in the colored sample, to 89.8 %. By the same time, the amount of  $\text{Cu}^{+2}$  atoms (as in the  $\text{CuO}$  black-colored oxide) decreased in the bleached sample and increased in the colored sample, correspondingly. Hence, it can be assumed that the electrochromic switching occurs due to the transition of only about 3.4 %  $\text{Cu}$  atoms (93.2–89.8 %) from  $\text{Cu}^{+}$  to  $\text{Cu}^{+2}$  and vice versa. This result is in agreement with the XRD patterns, revealing no detectable peaks of the  $\text{CuO}$  phase due to their relatively small quantity compared to those of the  $\text{Cu}_2\text{O}$  phase. Furthermore, the characteristic O1s peaks of the XPS spectrum were practically useless for the  $\text{CuO}$  and  $\text{Cu}_2\text{O}$  quantification because the O1s peak at 530.6 eV<sup>23</sup> can be associated with both the  $\text{CuO}$  and  $\text{Cu}_2\text{O}$  phases, while the peak at 531.6 eV can only be associated with the electrochromic inactive  $\text{Cu}(\text{OH})_2$  compound.

If one takes into account the crystallography data for the unit cells of cuprite- $\text{Cu}_2\text{O}$  and tenorite- $\text{CuO}$ , one can make an estimation of the possible variations in the volume that may induce the strain in the  $\text{Cu}_x\text{O}$  structure and, hence, invoke film degradation due to repeatable cycling. Under the assumption that the  $\text{Cu}_x\text{O}$  electrochromic behavior relies on only 3.4 % of the  $\text{Cu}$  atoms, we can estimate the relative changes in the crystallite volume, in which about 3.4 %  $\text{Cu}$  atoms from tenorite (a monoclinic structure with a unit cell volume  $V_c(\text{CuO}) = 81.03 \cdot 10^{-3} \text{ nm}^3$ <sup>19</sup>) recrystallize into cuprite (a cubic structure with a unit cell volume  $V_c(\text{Cu}_2\text{O}) = 77.83 \cdot 10^{-3} \text{ nm}^3$ <sup>20</sup>). One can assume that the crystallites within the film undergo a

negligible relative volume reduction during the coloration and a volume expansion during the bleaching. Hence, the limited cycling lifetime that was previously observed in these films<sup>17,18</sup> cannot be ascribed to the volume friction within the crystallites.

**Figures 4a to 4c** present the SEM micrographs of the surfaces of the as-prepared, bleached and colored films on the FTO substrates, correspondingly. The micrograph on **Figure 4a** reveals round grains of the as-prepared film with a diameter of about 250 nm. The grain size of the bleached films on **Figure 4b** seems similar. However, the micrograph of the colored-sample surface from **Figure 4c** reveals notably smaller round crystal grains.

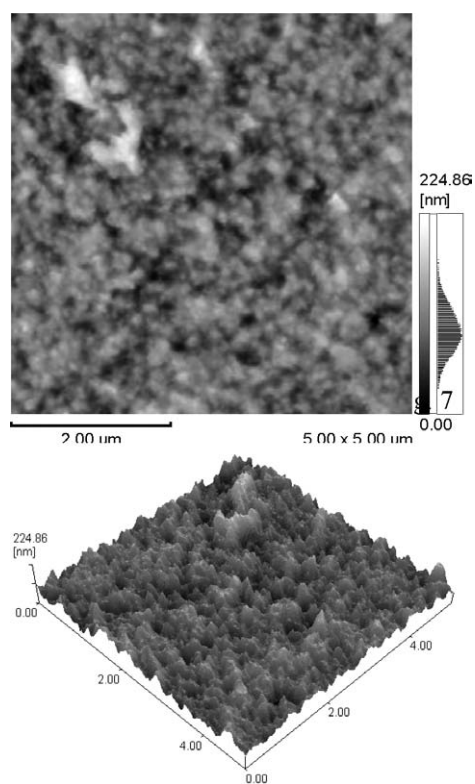


**Figure 7:** 2D and 3D surface images of FTO substrates

**Slika 7:** 2D- in 3D-posnetek površine FTO-podlage

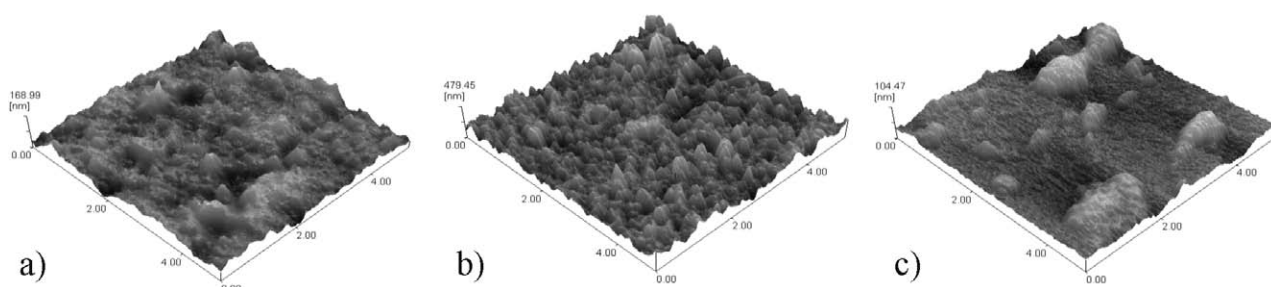


**Figure 8:** Three-dimensional surface images of  $\text{Cu}_x\text{O}$  thin films: a) as-prepared, b) colored and c) bleached  
**Slika 8:** Tridimenzionalen posnetek površine tanke plasti  $\text{Cu}_x\text{O}$ : a) pripravljeno, b) obarvano in c) obeljeno

Furthermore, as a consequence of the grain shrinkage, the porosity of the colored film seems to have increased notably (an obviously larger empty space among the grains upon the coloration). In addition, **Figure 5** shows the SEMs of: (a) the  $\text{Cu}_x\text{O}$  films deposited onto the glass (amorphous) substrate and (b) a profile of about 250 nm  $\text{Cu}_x\text{O}$  film on the glass substrate (the interface cross-section). From **Figure 5a** it is obvious that the  $\text{Cu}_x\text{O}$  film grows irregularly and non-homogeneously on an amorphous substrate, such as glass. However, the SEMs on **Figure 4**, along with the XRD patterns, showed a mixed amorphous-crystalline growth on the crystalline substrate (FTO).

Two-dimensional AFM surface images of the as-prepared, bleached and colored  $\text{Cu}_x\text{O}$  thin films are presented in **Figure 6**. For a comparison, **Figure 7** includes 2D and 3D surface images of the FTO substrate. The scale of all the three images is 5  $\mu\text{m}$ . As can be seen from **Figure 6**, there are significant differences between the surfaces of the as-prepared, bleached and colored samples. In addition, from **Figure 8** one can see that the electrochemical voltage cycling notably affects the surface roughness. In other words, the oxidation process (coloration), taking place on a sample surface, deteriorates the surface smoothness, increasing the root-mean-square roughness. On the other hand, the reduction

process (bleaching) is followed by an improvement of the surface smoothness. Furthermore, the roughness parameter ( $R_q$ ) derived from the AFM scans of the observed surfaces (an area of 5  $\mu\text{m} \times 5 \mu\text{m}$ ) decreased from 480 nm for the colored to 108 nm for the bleached sample.

In order to compare the compositional homogeneity of the  $\text{Cu}_x\text{O}$  thin films in their as-prepared, colored and bleached state, their phase surface images are presented on **Figure 9**, correspondingly. Besides  $\text{Cu}_2\text{O}$  and  $\text{CuO}$ , some minor amounts of  $\text{Cu}(\text{OH})_2$  were found in all three samples. Furthermore, the results showed that the cuprite ( $\text{Cu}_2\text{O}$ ) phase is the most abundant in the bleached state, which is in agreement with the XPS results of this study. Comparing the phase images of the as-prepared and colored states, it could be concluded that the amount of the tenorite ( $\text{CuO}$ ) phase is comparable in both the as-prepared and colored states which is again in line with the XPS results.

#### 4 CONCLUSION

The coloration process of the chemically deposited  $\text{Cu}_x\text{O}$  films can be considered as a reversible transfer of the film 3–4 % of the total 90 %  $\text{Cu}^{+1}$  into  $\text{Cu}^{+2}$ . The coloration can thus be attributed to a decrease of 3–4 %

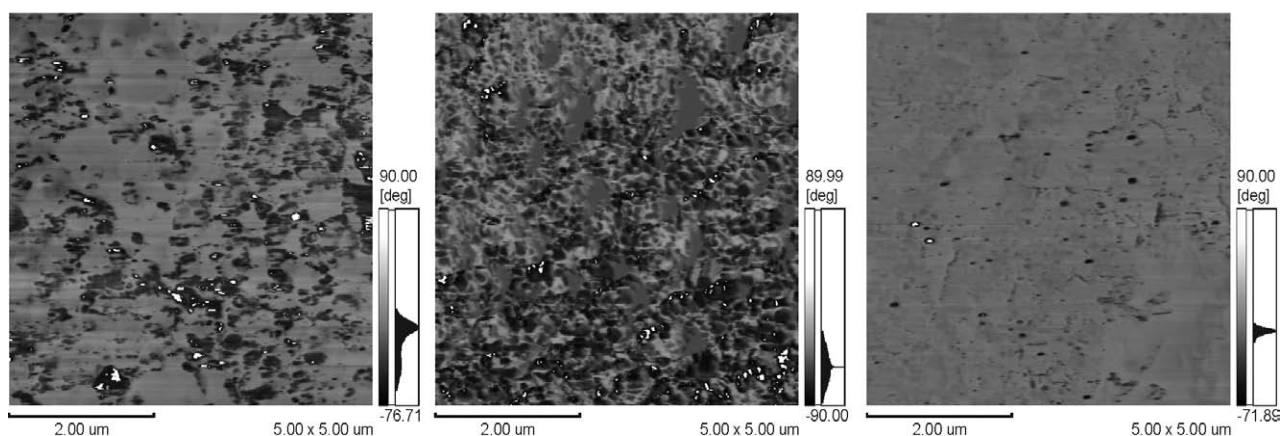


**Figure 9:** Phase surface images of  $\text{Cu}_x\text{O}$  thin films: a) as-prepared, b) colored and c) bleached. The scale is 5  $\mu\text{m}$  in both directions and 90 nm in height.

**Slika 9:** Površinska slika faz v tanki plasti  $\text{Cu}_x\text{O}$ : a) pripravljeno, b) obarvano in c) obeljeno. Merilo je 5  $\mu\text{m}$  v obeh smereh in 90 nm po višini.

of the interstitial oxygen, creating oxygen vacancies in the  $\text{CuO}$  film. From all the above findings, it appears that only 3–4 % of the copper atoms in the film surface represent the coloration centers that are driven to switch the transmittance between 30 % and 80 %<sup>17,18</sup>. The SEM micrographs showed that the grain size of the  $\text{Cu}_x\text{O}$  crystallites notably shrank upon the coloration of the film, whereas the porosity grew up. Significant changes in the surface morphology among the as-prepared and treated samples were also detected by AFM. While the oxidation process (the coloring) deteriorated the surface smoothness, the reduction (the bleaching) invoked the surface smoothing. The AFM phase imaging revealed the existence of three different phases in the as-deposited, colored and bleached films:  $\text{Cu}_2\text{O}$ ,  $\text{CuO}$  and a minor amount of the hydroxide phase –  $\text{Cu}(\text{OH})_2$ . In agreement with the XPS results, the amount of the dominant cuprite phase was found to be the highest for the bleached state, while the tenorite phase ( $\text{CuO}$ ) appeared in comparable amounts in the as-prepared and the colored states. The limited quantity of the electrochromic active Cu-atoms within the thin  $\text{Cu}_x\text{O}$  films on the transparent conductive oxide (TCO) limits its performance in the white-light-transmittance modulation between 20 % and 80 %. If the  $\text{Cu}_x\text{O}$  films are sensitized as nanocrystals within a TCO matrix, it can be expected that a more efficient coloration can be achieved.

## 5 REFERENCES

- <sup>1</sup> C. G. Granqvist, Handbook of Inorganic Electrochromic Materials, Elsevier, Amsterdam 1995
- <sup>2</sup> J. I. Pankove, Display Devices, Springer, Berlin 1980
- <sup>3</sup> C. M. Lampert, T. R. Omstead, P. C. Yu, Sol. Energy Mater., 14 (1986), 161–174, doi:10.1016/0165-1633(86)90043-2
- <sup>4</sup> A. E. Rakhshani, J. Appl. Phys., 62 (1987), 1528–1529, doi:10.1063/1.339619
- <sup>5</sup> N. Ozer, F. Tepehan, Sol. Energy Mater. Sol. Cells, 30 (1993), 1–26, doi:10.1016/0927-0248(93)90027-Z
- <sup>6</sup> H. Demiryont, US Patent No. 4830471, 16 May 1989
- <sup>7</sup> F. I. Brown, S. C. Schulz, US Patent No. 5585959, 17 Dec. 1996
- <sup>8</sup> T. J. Richardson, J. L. Slack, M. R. Rubin, Electrochim. Acta, 46 (2001), 2281–2284, doi:10.1016/S0013-4686(01)00397-8
- <sup>9</sup> M. E. Abu-Zeid, A. E. Rakhshani, A. A. Al-Jassar, Y. A. Youssef, Phys. Stat. Solidi (A), 93 (1986), 613–620, doi:10.1002/pssa.2210930226
- <sup>10</sup> V. Georgieva, M. Ristov, Sol. Energy Mater. Sol. Cells, 73 (2002), 67–73, doi:10.1016/S0927-0248(01)00112-X
- <sup>11</sup> S. C. Ray, Sol. Energy Mater. Sol. Cells, 68 (2001), 307–312, doi:10.1016/S0927-0248(00)00364-0
- <sup>12</sup> W. M. Sears, E. Fortin, Sol. Energy Mater., 10 (1984), 93–103, doi:10.1016/0165-1633(84)90011-X
- <sup>13</sup> E. Fortin, D. Masson, Solid-State Electron., 25 (1982), 281–283, doi:10.1016/0038-1101(82)90136-8
- <sup>14</sup> A. Roos, T. Chibuye, B. Karlsson, Sol. Energy Mater., 7 (1983), 453–465, doi:10.1016/0165-1633(83)90018-7
- <sup>15</sup> M. Ristov, Gj. Sinadinovski, I. Grozdanov, Thin Solid Films, 123 (1985), 63–67, doi:10.1016/0040-6090(85)90041-0
- <sup>16</sup> M. Ristova, J. Velevska, M. Ristov, Sol. Energy Mater. Sol. Cells, 71 (2002), 219–230, doi:10.1016/S0927-0248(01)00061-7
- <sup>17</sup> R. Neskovska, M. Ristova, J. Velevska, M. Ristov, Thin Solid Films, 515 (2007), 4717–4721, doi:10.1016/j.tsf.2006.12.121
- <sup>18</sup> M. Ristova, R. Neskovska, V. Mirceski, Sol. Energy Mater. Sol. Cells, 91 (2007) 14, 1361–1365, doi:10.1016/j.solmat.2007.05.018
- <sup>19</sup> Powder Diffraction File No. 4680, CPDS International Center for Diffraction Data, Newtown Square, 2006
- <sup>20</sup> Powder Diffraction File No. 1104, CPDS International Center for Diffraction Data, Newtown Square, 1985
- <sup>21</sup> Powder Diffraction File No. 778, CPDS International Center for Diffraction Data, Newtown Square, 1975
- <sup>22</sup> G. E. Muilenberg (Ed.), Handbook of X-ray photoelectron spectroscopy, Perkin – Elmer Corporation, 1979
- <sup>23</sup> XPS Handbook of elements and native oxides, XPS International Incorporated, 1999
- <sup>24</sup> T. Ghodselahi, M. A. Vesaghi, A. A. Shafiekhani, A. Baghizadeh, M. Lameii, Applied Surface Science, 255 (2008), 2730–2734, doi:10.1016/j.apsusc.2008.08.110
- <sup>25</sup> I. G. Casella, M. Gatta, Journal of Electroanalytical Chemistry, 494 (2000), 12–20, doi:10.1016/S0022-0728(00)00375-2